Thermoflow Multiplicity in a Packed-Bed Reactor: Conduction and Cooling Effects

Steady states with different flow rates and temperature profiles may exist in different tubes of a multitube packed-bed reactor due to the coupling among the species, energy and momentum balances, and the change of physical properties with temperature and pressure. Under typical operating conditions if no axial conduction of heat occurs thermoflow multiplicity can be found only for unrealistically high heats of reaction and/or over a very narrow range of exit pressures. However, accounting for the finite but small heat conduction in the reactor tubes leads to multiplicity for typical parameters and a reasonable range of exit pressures. Cooling tends to decrease the region of parameters for which the multiplicity occurs.

Jorge Pita
Vemuri Balakotaiah
Dan Luss
Department of Chemical Engineering
University of Houston
Houston, TX 77004

Introduction

Steady states with different flow rates may exist under the same overall pressure gradient in many systems. This *thermoflow multiplicity* is caused by the interaction among the species, energy and momentum balances, and a sensitive dependence of the physical properties on the state of the system. Recent studies (Matros and Chumakova, 1980; Lee, et al., 1987, 1988) showed that this multiplicity may be found when a single reaction is carried out in an adiabatic, multitube, packed-bed reactor. A pseudohomogeneous plug-flow model, which ignores axial dispersion, predicts that for a gaseous mixture the multiplicity occurs for a rather high and unrealistic adiabatic temperature rise. A reaction-induced increase in the number of moles shifts the multiplicity region to lower and more realistic values of the adiabatic temperature rise. This model, which ignores axial dispersion of heat, predicts that a unique steady state exists for any set of parameters if the inlet velocity is specified. Thus, it clearly points out the intrinsic difference between thermoflow and thermokinetic multiplicity.

In practice, multitube reactors are cooled, and the axial dispersion of heat can affect their qualitative behavior. We determine here the impact of these two phenomena on the multiplicity features of a multitube reactor and examine if thermoflow multiplicity can be found under practical operating conditions. The general model contains a very large number of parameters so that its analysis and presentation of results are rather cumbersome. Thus, we analyze first limiting, simplified models and then compare their predictions with those of the general model. This approach yields important insight into the behavioral features of this important industrial reactor and the conditions under which thermoflow multiplicity can be found.

Development of a Mathematical Model

Consider a cooled, multitube packed-bed reactor in which a single, irreversible, exothermic, $A \rightarrow B$ chemical reaction occurs. The pressure drop across the bed is specified and determines the flow rate in the tubes. We describe each tube by a pseudohomogeneous, one-dimensional, plug-flow model that accounts for axial dispersion of heat. The steady-state continuity, species, energy and momentum balances are:

$$\frac{d}{dz}(\rho u) = 0 \tag{1}$$

$$\frac{d}{dz}(uC_A) = -r \tag{2}$$

$$\lambda_e \frac{d^2T}{dz^2} - \rho u c_p \frac{dT}{dz} + (-\Delta H)r - \frac{2}{R_t} h(T - T_w) = 0 \tag{3}$$

$$\frac{dP}{dz} + \rho u \frac{du}{dz} = -f_p \tag{4}$$

The frictional pressure drop f_p is computed by the Ergun equation

$$f_p = A\mu u + B(\rho u)u$$

where the constants A and B depend on the properties of the packing. The corresponding boundary conditions are

$$P = P_o,\ C_A = C_{A_o} \quad z = 0 \tag{6}$$

$$\rho_o u_o c_p T_o - \rho u c_p T = -\lambda_e \frac{dT}{dz} \quad z = 0 \tag{7}$$

$$\frac{dT}{dz} = 0,\ P = P_1 \quad z = L \tag{8}$$

Assuming that the gaseous mixture satisfies the ideal gas-law, the momentum balance (Eq. 4) can be brought to the form (Lee et al., 1987)

$$\left[1 - \frac{\rho_o u_o^2}{P_o}\frac{T}{T_o}\left(\frac{P_o}{P}\right)^2\right]\frac{dP}{dz} + \frac{\rho_o u_o^2}{T_o}\left(\frac{P_o}{P}\right)\frac{dT}{dz} = -(A\mu u + B\rho u^2) \tag{9}$$

Under practical conditions, the term $\rho_o u_o^2/P_o$ is much smaller than unity. Thus, to simplify the analysis we omit this term in the bracket multiplying dP/dz. We also assume that the viscosity of the mixture is independent of pressure and conversion and increases with temperature according to the relation

$$\mu = \mu(T_o)\left(\frac{T}{T_o}\right)^{0.5} \tag{10}$$

To simplify the algebraic manipulations required to determine the structure of the solutions we assume that the chemical reaction is of order zero, i.e.,

$$r(C, T) = k(T)H(C) = k(T_o)X(y)H(C) \tag{11}$$

where H is the Heaviside's function and

$$y = \frac{T}{T_o} \tag{12}$$

$$X(y) = \frac{k(T)}{k(T_o)} = \exp\left[\frac{E}{RT_o}\left(1 - \frac{1}{y}\right)\right] \tag{13}$$

Introducing the dimensionless variables

$$\Pi = \frac{P}{P_o} \qquad s = \frac{z}{L}$$

$$y_w = \frac{T_w}{T_o} \qquad x = \frac{u_o C_{A_o} - u C_A}{u_o C_{A_o}}$$

$$\gamma = \frac{E}{RT_o} \qquad Da = \frac{k(T_o)L}{u_o C_{A_o}}$$

$$\beta = \frac{(-\Delta H)C_{A_o}}{\rho_o c_p T_o} \qquad \alpha = \frac{2hT_o}{R_t k(T_o)(-\Delta H)}$$

$$\phi_h^2 = \frac{k(T_o)L^2\rho_o c_p}{\lambda_e C_{A_o}} \qquad E_1 = \frac{A\mu(T_o)k(T_o)L^2}{P_o C_{A_o}}$$

$$E_2 = \frac{B\rho_o k(T_o)^2 L^3}{P_o C_{A_o}^2} \qquad E_3 = \frac{\rho_o k(T_o)^2 L^2}{P_o C_{A_o}^2} \tag{14}$$

the species, momentum and energy balances can be written in the form

$$\frac{dx}{ds} = Da\, X(y)\, H(1 - x) \tag{15}$$

$$\Pi\frac{d\Pi}{ds} = -\frac{E_1 y^{1.5}}{Da} - \frac{E_2 y}{Da^2} - \frac{E_3}{Da^2}\frac{dy}{ds} \tag{16}$$

$$\frac{Da}{\phi_h^2}\frac{d^2y}{ds^2} - \frac{dy}{ds} + \beta Da\,[X(y)H(1 - x) - \alpha(y - y_w)] = 0 \tag{17}$$

subject to the boundary conditions

$$x(0) = 0 \tag{18}$$

$$\Pi(0) = 1; \quad \Pi(1) = \Pi_1 \tag{19}$$

$$\frac{Da}{\phi_h^2}\frac{dy(0)}{ds} = y(0) - 1; \quad \frac{dy(1)}{ds} = 0 \tag{20}$$

For any specified set of parameters (γ, β, ϕ_h^2, α, y_w, E_1, E_2, E_3) there exists at most a few values of Da, which is proportional to $1/u_o$, satisfying the three Eqs. 15–17 and the corresponding boundary conditions (Eqs. 18–20). In other words, there exist at most several feasible inlet velocities under any specified pressure drop.

In examining Eqs. 15–17 we note that the terms E_1 and E_2 are associated with the laminar and turbulent frictional pressure drop, respectively, The term E_3 is associated with the pressure change due to the thermal expansion of the gaseous mixture. In general, the turbulent friction is the major cause of pressure change. The ratio E_2/E_3 is equal by definition to BL. Its value is usually at least 10^4 as B is of the order of 100 cm^{-1}. The ratio E_2/E_1 is usually larger than unity and a typical value is of the order of 10. The parameter ϕ_h^2/Da is the heat Peclet number, Pe_h, which is the ratio between the characteristic axial conduction time ($t_\lambda = L^2\rho_o c_p/\lambda_e$) and the convection time ($t_c = L/u_o$). We express the heat dispersion by the ratio ϕ_h^2/Da to point out its dependence on the Da number, i.e., the inlet velocity.

Inspection of Eq. 17 indicates that the temperature in a tube will remain constant at $y = 1$ until all the reactant is exhausted and decreases monotonically thereafter if

$$\alpha = \alpha_i \triangleq \frac{1}{1 - y_w} \tag{21}$$

or equivalently if

$$y_w = y_{wi} \triangleq 1 - 1/\alpha \tag{22}$$

If $\alpha > \alpha_i$ or $y_w < y_{wi}$, the reactor is overcooled and the temperature decreases monotonically in the flow direction. We do not consider these unpractical situations, for which a unique solution exists.

We analyze first two limiting models of very large and very small Peclet heat numbers, and study later the general model.

Negligible-Dispersion Model: $Pe_h \to \infty$

When the characteristic convection time is much smaller than that for the axial conduction of heat, i.e., $\phi_h^2/Da = Pe_h$ is very large, it is common practice to ignore the conduction (first) term in the energy balance (Eq. 17) and reduce it to

$$\frac{dy}{ds} - \beta Da[X(y)\, H(1-x) - \alpha(y - y_w)] = 0 \qquad (23)$$

and boundary condition (Eq. 20) is replaced by

$$y(0) = 1 \qquad (24)$$

The set of equations (Eqs. 15, 16, and 23) subject to boundary conditions (Eqs. 18, 19, and 24) defines the limiting *negligible dispersion model.*

We consider first the case in which the conversion in the reactor is not complete, i.e., $x < 1$ at the exit. Integrating Eq. 23 we find that

$$\beta Da - I(y_1, 0) = 0 \qquad (25)$$

where we define

$$I(y_1, n) = \int_1^{y_1} \frac{y^n\, dy}{X - \alpha(y - y_w)} \qquad (26)$$

Dividing Eq. 16 by Eq. 23 and integrating we get the steady-state equation

$$F_1(Da, \Lambda_j, \mathbf{p}) = \frac{1}{\Lambda_j} - \frac{2E_1/E_j}{\beta Da^2} I(y_1, 1.5) - \frac{2E_2/E_j}{\beta Da^3} I(y_1, 1) - \frac{2E_3/E_j}{Da^2}(y_1 - 1) = 0 \qquad (27)$$

where

$$\Lambda_j = \frac{E_j}{1 - \Pi_1^2} \quad j = 1, 2, 3 \qquad (28)$$

In solving Eq. 27 one uses Eq. 25 to determine the monotonic dependence of y_1 on βDa.

Next we consider the case in which the conversion is complete. Dividing Eq. 23 by Eq. 15 and integrating, we find that at s_c, the point at which the conversion is complete

$$\beta = \int_1^{y_c} \frac{X\, dy}{X - \alpha(y - y_w)}. \qquad (29)$$

The smallest Da (largest inlet velocity) for which the conversion is complete, $D\overset{*}{a}$, satisfies the relation

$$\beta D\overset{*}{a} = I(y_c, 0) \qquad (30)$$

When $Da > D\overset{*}{a}$, we find by integrating Eq. 23 from s_c to $s = 1$ that the exit temperature satisfies the equation

$$\alpha\beta Da(1 - s_c) = \ln \frac{y_c - y_w}{y_1 - y_w} \qquad (31)$$

The corresponding steady-state equation, obtained by integrating $d\Pi^2/dy$ first from $y = 1$ to y_c and then from y_c to y_1, is

$$F_2(Da, \Lambda_j, \mathbf{p}) = \frac{1}{\Lambda_j} - \frac{2E_1/E_j}{\beta Da^2}\left[I(y_c, 1.5) - \frac{K(y_1, 1.5)}{\alpha}\right] - \frac{2E_2/E_j}{\beta Da^3}\left[I(y_c, 1) - \frac{K(y_1, 1)}{\alpha}\right] - \frac{2E_3/E_j}{Da^2}(y_1 - 1) = 0 \qquad (32)$$

where

$$K(y_1, n) = \int_{y_c}^{y_1} \frac{y^n\, dy}{y - y_w} \qquad (33)$$

Thus, the steady-state equation is of the form

$$F(Da, \Lambda_j, p) = \begin{cases} F_1 = 0 & Da \le D\overset{*}{a} \\ F_2 = 0 & Da > D\overset{*}{a} \end{cases} \qquad (34)$$

F has the following properties:

1. It is continuous for all $Da > 0$.
2. dF/dDa is discontinuous at $Da = D\overset{*}{a}$ unless $E_3 = 0$.
3. d^mF/dDa^m is discontinuous at $Da = D\overset{*}{a}$ for all $m \ge 2$.

The boundaries of the region of (γ, β) values for which multiplicity exists for some specified pressure drop, or equivalently Λ_j, can be found by the technique described by Lee et al. (1987). We present here mainly the results of the analysis and refer readers interested in the algebraic manipulations to Pita (1988).

The method described by Lee et al. (1987) can be used to show that for any specified α, y_w and two ratios E_i/E_j a unique solution exists for any Λ_j for all (γ, β) to the left of a g (hysteresis) curve which consists, in general, of two segments. The first, denoted as g^*, always exists and satisfies the conditions

$$\frac{dF_1}{dDa}(D\overset{*}{a}) = 0 \qquad (35a)$$

and

$$F(D\overset{*}{a} - \epsilon)F(D\overset{*}{a} + \epsilon) < 0. \qquad (35b)$$

The second, denoted as H^*, does not exist in some cases, and is a horizontal line in the (γ, β) plane (γ = constant) which satisfies the conditions

$$\frac{dF_1}{dDa} = \frac{d^2F_1}{dDa^2} = 0. \qquad (36)$$

Calculations show that this line exists (when it does) only for β values much larger than those encountered in practice, so that it usually need not be found for this model.

Figures 1a–c and 2a–c show the dependence of the g (hysteresis) curves for three limiting cases on α and y_w. Figures 1a and 2a describe the case in which $E_2 = E_3 = 0$, so that the pressure drop is due to the laminar friction term. Figures 1b and 2b are for the case of $E_1 = E_3 = 0$, for which the pressure change is due to the turbulent friction term in the Ergun equation. Figures 1c and 2c are of the case in which $E_1 = E_2 = 0$ so that the pressure drop is caused by the thermal expansion of the gas.

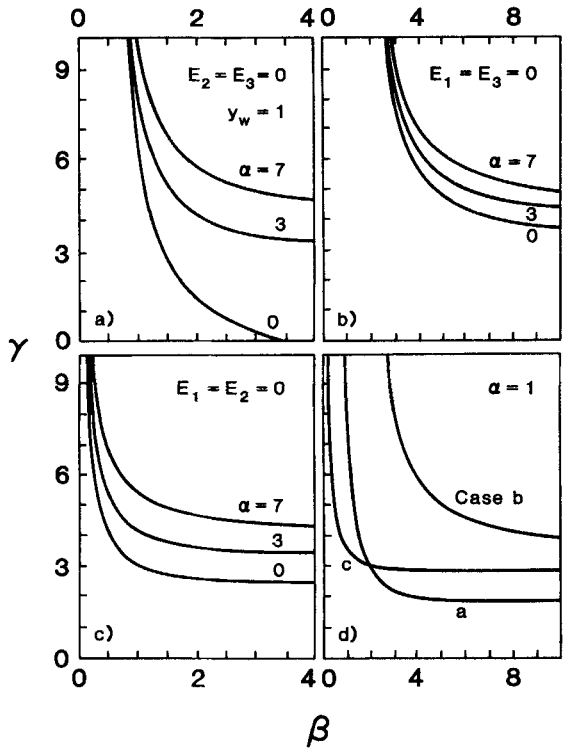

Figure 1. a–c, dependence of the uniqueness boundary on the cooling parameter α for a cooled reactor for the three limiting cases for the negligible dispersion model; d, curves for $\alpha = 1$. In all the cases, $y_w = 1$.

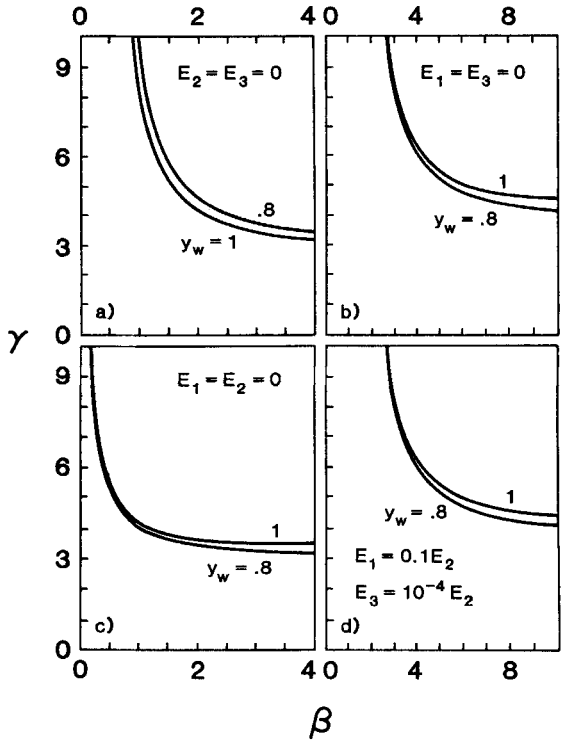

Figure 2. Dependence of the uniqueness boundary on the cooling temperature: a–c, limiting cases; d, general case for the negligible dispersion model. In all four cases, $\alpha = 3$.

In all the three limiting cases, increasing the heat transfer coefficient shifts the g^* curve to the right, i.e., increases the region of (γ, β) values for which a unique solution exists for any Λ_j. The heat transfer coefficient α has a very strong impact on the g curves for the laminar case (Figure 1a) and a smaller impact on the g curves for the turbulent (Figure 1b) and thermal expansion (Figure 1c) cases. Figure 2 shows that decreasing the coolant temperature has only a very small impact on the location of the g curves, shifting them slightly to higher γ values in the laminar case (Figure 2a), and to slightly lower γ values for the turbulent (Figure 2b), thermal expansion (Figure 2c) and the general case (Figure 2d). The calculations show that for the thermal expansion case the trend is reversed for high γ values, i.e., decreasing the coolant temperature shifts the g curves to slightly higher γ values.

Figure 1 shows that the sufficient conditions for uniqueness for all Λ_i for the adiabatic case ($\alpha = 0$) derived by Lee et al. (1987), are valid also with cooling ($\alpha > 0$). Thus, we can immediately write down the following sufficient conditions for uniqueness for all Λ_i

$$\beta < 0.587 \quad \text{when } E_2 = E_3 = 0 \tag{37}$$

$$\beta < 2 \quad \text{when } E_1 = E_3 = 0 \tag{38}$$

$$\gamma\beta < 1.256, \text{ provided } y_w \leq 1 \quad \text{when } E_1 = E_2 = 0 \tag{39}$$

When only for the thermal expansion is accounted for ($E_1 = E_2 = 0$) a bound stronger than Eq. 39 can be found when $\alpha \neq 0$ and $y_w \neq 1$, by solving the equation

$$\frac{2\alpha(1 - y_w)\theta}{\exp(\theta) - \alpha(1 - y_w)} = \ln \frac{1 - \alpha(1 - y_w)\exp(-\theta)}{1 - \alpha(1 - y_w)} \tag{40}$$

for θ and computing the asymptotic value of $\gamma\beta$ from the relation

$$\gamma\beta = \ln\left[\frac{\exp(\theta) - \alpha(1 - y_w)}{1 - \alpha(1 - y_w)}\right]. \tag{41}$$

Calculations indicate that the limiting value is a monotonic increasing function of α and a decreasing function of y_w. For example, for $\alpha = 7$ and $y_w = 0.9$, Eq. 41 predicts the asymptotic boundary $\gamma\beta = 1.4$.

In the general case the g^* and H^* curves are bounded by those obtained for the three limiting models. Figure 1d shows the three curves for the case $\alpha = y_w = 1$. It is seen that the g^* and H^* for the general case are bounded from above by the curve for the limiting turbulent case ($E_1 = E_3 = 0$) and from below by that for the thermal expansion case ($E_1 = E_2 = 0$) for small β and that for the laminar pressure drop for large β. We conclude that the limiting models are very useful for deriving conservative uniqueness boundaries. Figure 2d shows that decreasing the coolant temperature in the general case has only a minor impact on the location of the g curves, shifting them to the left (lower γ value). In this and all other simulations of the general case we used $E_1 = 0.1\ E_2$ and $E_3 = 10^{-4}\ E_2$.

The region of (γ, β) values for which multiplicity exists is

bounded on one side by the g curve and on the other side by the BLS_1 curve, which is the set of (γ, β) values for which the ignition point occurs for the lowest allowable exit pressure Π_l, or equivalently for the lowest possible value of Λ_j, denoted Λ_{jl}. To find this set, one selects a γ value and solves simultaneously the steady-state equations (Eqs. 25 and 27) and

$$0.5Da^2\frac{dF_1(y_1)}{dDa} = E_1/E_j\left(\frac{2I(y_1, 1.5)}{\beta Da} - y_1^{1.5}\right) + \frac{E_2/E_j}{Da}\left(\frac{3I(y_1, 1)}{\beta Da} - y_1\right) + \beta E_3/E_j\left\{\frac{2(y_1 - 1)}{\beta Da} - [X(y_1) - \alpha(y_1 - y_w)]\right\} = 0 \quad (42)$$

for y_1, β and Da for the specified limiting Λ_{jl}. Numerical calculations show that the cooling shifts the BLS_1 only slightly to the right (larger β value) for the three limiting cases.

In practice the turbulent pressure term is the main cause of pressure loss and $E_2 \gg E_1 \gg E_3$. The BLS_1 for the general case is very similar to that found for the turbulent case and is shifted to slightly higher β values with increasing α and decreasing y_w values. The g curve is very close to that of the turbulent case for large β value. However, for small β values it tends towards that for the thermal expansion case no matter how small E_3 is. Thus, in the general case it is possible to obtain thermoflow multiplicity for β values much smaller than those for the turbulent case (Figure 3). That figure shows also the g curve for the turbulent case (dashed line). The BLS_1 curves are practically the same for both cases. The graph shows that thermoflow multiplicity may be found for any (γ, β) values to the left of the g curve for the turbulent case. Thus, even though E_1 and E_3 are much smaller than E_2, the laminar friction term and thermal expansion have a strong impact on the boundary of the (γ, β) values for which this multiplicity may exist.

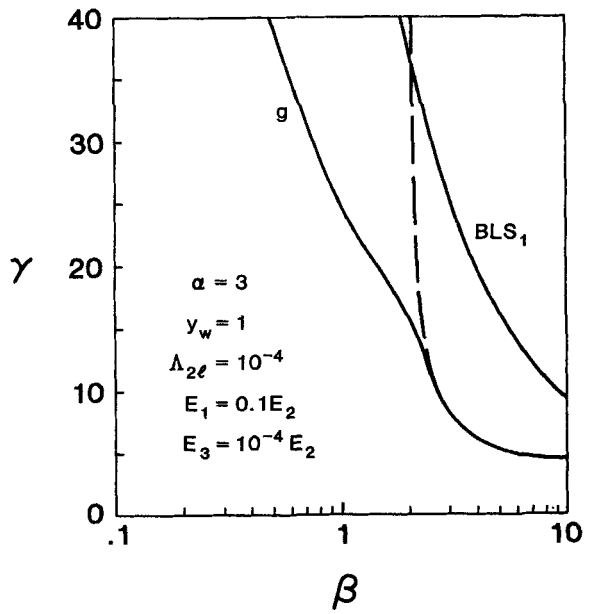

Figure 3. Region of (γ, β) values for which thermoflow multiplicity exists for $\Lambda_{2l} = 10^{-4}$. Dashed line is the g curve for the turbulent case.

The ratio of Λ_2 at ignition to Λ_2 at extinction tends to increase with increasing β values within the multiplicity region. For example, for $\gamma = 20$ and $\alpha = 0$, this ratio is 1.0003, 1.0014, and 1.0484 for β values of 1, 2, and 5, respectively. Thus, the region of admissible pressure drops for which multiplicity occurs is very narrow and increases with an increase in the adiabatic temperature rise for a fixed γ value. We conclude that according to the negligible dispersion model the likelihood of finding thermoflow multiplicity under practical conditions is very small. It is of interest to check if other models lead to different predictions.

Lumped-Thermal Model: $Pe_h \to 0$

When the characteristic time for axial conduction is much smaller than that for convection, i.e., $Pe_h \to 0$, the temperature in the reactor is essentially uniform. Under these conditions integration of Eqs. 15 and 17 give the following relations for the conversion and dimensionless temperature

$$x(s) = \begin{cases} DaX(y)s & \text{for } DaX(y)s \le 1 \quad (43a) \\ 1 & \text{for } DaX(y)s > 1 \quad (43b) \end{cases}$$

$$y - 1 = \begin{cases} \beta Da[X(y) - \alpha(y - y_w)] & \text{if } DaX(y) \le 1 \quad (44a) \\ \beta[D\mathring{a}X(y) - \alpha Da(y - y_w)] & \text{if } DaX(y) > 1 \quad (44b) \end{cases}$$

Using Eq. 43a we find that

$$D\mathring{a} = 1/X(y_c) \quad (45)$$

where y_c, the temperature at $Da = D\mathring{a}$, has to satisfy the following relation, obtained by substitution of Eq. 45 into Eq. 44a

$$y_c - 1 = \beta[1 - \alpha(y_c - y_w)/X(y_c)] \quad (46)$$

By integrating the momentum balance Eq. 16 we obtain the steady-state equation

$$F(Da, \Lambda_j, \mathbf{p}) = \frac{1}{\Lambda_j} - \frac{2E_1/E_j}{Da}y^{1.5} - \frac{2E_2/E_j}{Da^2}y - \frac{2E_3/E_j}{Da^2}(y - 1) = 0 \quad (47)$$

where Eq. 44 determines the relation between y and Da. This dependence for $Da \le D\mathring{a}$ (Eq. 44a) differs from that for $Da > D\mathring{a}$ (Eq. 44b).

It should be noted that for some γ and β values Eq. 44a exhibits *thermokinetic multiplicity*, i.e., three solutions exist for the same Da values. The boundary of this region of (γ, β) values consists of two sections which intersect at $\beta = \beta^*$. For all $\beta > \beta^*$, the boundary is the line $\gamma = \gamma^*$, where γ^* satisfies the equation

$$(4/\gamma^* - 1)\exp(\gamma^* - 2) - \alpha(1 - y_w) = 0 \quad (48)$$

The second section is found by selecting some $\gamma > \gamma^*$, solving

$$\frac{dy_c}{dDa} = X(y_c) - \alpha(y_c - y_w) - (y_c - 1)\left[\frac{\gamma}{y_c^2}X(y_c) - \alpha\right] = 0 \quad (49)$$

and computing from Eq. 46 the corresponding β. The value of β^* corresponds to y_c computed by Eq. 49 for $\gamma = \gamma^*$. In the special case of an adiabatic reactor ($\alpha = 0$) $\beta^* = 1$ and the uniqueness boundary is the curve

$$\gamma = \frac{(1+\beta)^2}{\beta} \quad \beta < 1 \tag{50a}$$

$$\gamma = 4 \quad \beta \geq 1 \tag{50b}$$

Multiple solutions exist for some Da for all (γ, β) to the right of this boundary.

Figures 4a–c and 5a–c show the dependence of the g^* curves on α and y_w for the same limiting cases shown for the negligible dispersion model in Figures 1 and 2. These limiting cases are of situations in which we account only for the pressure drop due to either the laminar or the turbulent term in the Ergun equation, or the thermal expansion of the gaseous mixture. As in the negligible dispersion model, increasing the heat transfer coefficient shifts these curves to the right (Figure 4), increasing the region of (γ, β) values for which uniqueness exists for all Λ_j. The impact of changes in the heat transfer coefficient, α, is much stronger than that of changes in the coolant temperature, y_w (Figure 5), which is qualitatively the same as in the neglibile dispersion model. The sufficient conditions for uniqueness for the adiabatic case are sufficient also for all the cooled cases.

The g curves for this model are always to the left of those for the negligible dispersion model. Thus, the thermal dispersion introduces the multiplicity at lower β values. To illustrate the computations of these g curves consider the laminar limiting

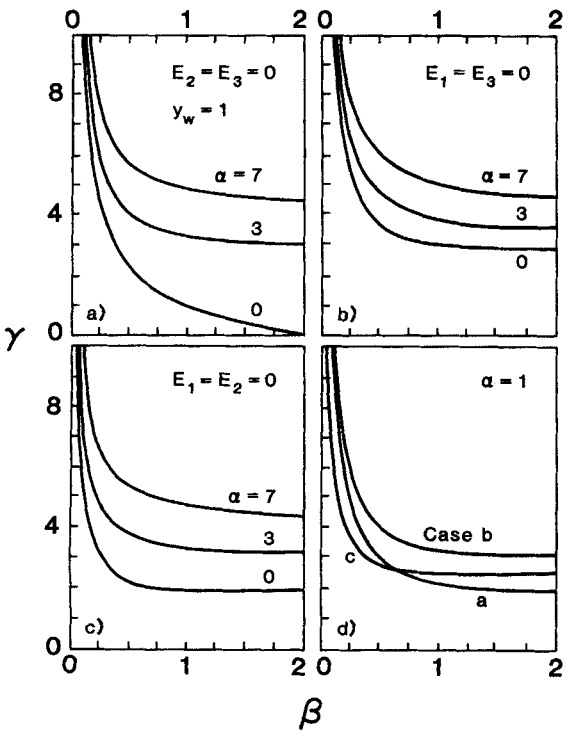

Figure 4. a–c, dependence of the uniqueness boundary on the cooling parameter α for a cooled reactor for the three limiting cases for the lumped-thermal model; d, curves for $\alpha = 1$. In all cases, $y_w = 1$.

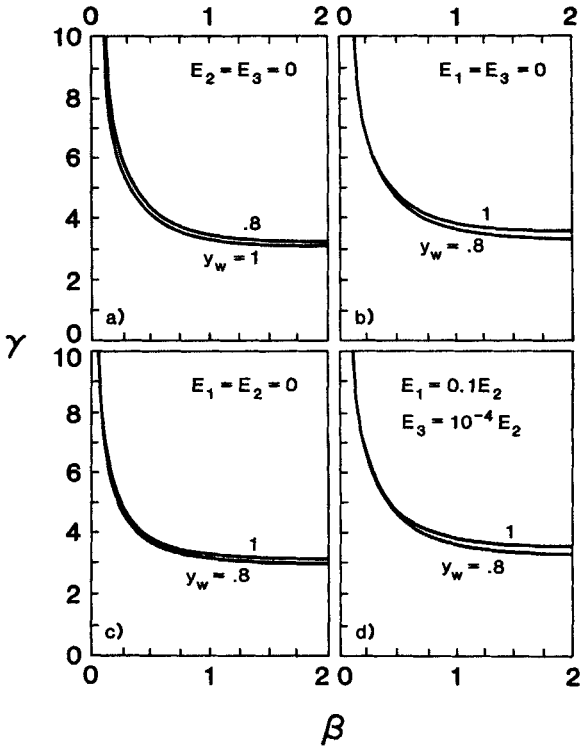

Figure 5. Dependence of the uniqueness boundary on the cooling temperature: a–c, limiting cases; d, general case for the lumped-thermal model. In all four cases, $\alpha = 3$.

case of $E_2 = E_3 = 0$. By differentiation of Eq. 47 and use of Eq. 44a we find that $dF(y_c)/dDa$ vanishes if

$$2y_c(y_c - 1)\left[\frac{\gamma}{y^2}X(y_c) - \alpha\right] - (3 - y_c)\,[X(y_c) - \alpha(y_c - y_w)] = 0 \tag{51}$$

The g^* curve is found by a simultnaeous solution of Eqs. 51 and 46 for a specified α and y_w. For the adiabatic case, the uniqueness boundary (g^* curve) is given by

$$\gamma = \frac{(1+\beta)(2-\beta)}{2\beta} \tag{52}$$

For the nonadiabatic case, the g^* curves for large γ values approach the adiabatic asymptote

$$\gamma\beta = 1 \tag{53}$$

Thus, multiplicity can occur in this case for very small β values, in contrast to the negligible dispersion model for which condition 37 guarantees uniqueness for all $\beta < 0.587$. The g^* curve intersects the $\gamma = 0$ axis for all

$$\alpha < \frac{1}{25 - y_w} \tag{54}$$

In these cases multiplicity can occur even if the rate constant is independent of the temperature. In the adiabatic case ($\alpha = 0$)

the g^* curve intersects the γ axis at $\beta = 2$, while in the negligible dispersion model it did so at $\beta = 3.6$. This is another indication of the shift of the g^* curve to lower β values by the axial dispersion of heat. For all α values which do not satisfy condition 54 an H^* curve (γ = constant) exists for all β values larger than some critical value.

Similarly, it can be shown that in the limiting turbulent pressure drop case (Figures 4b and 5b) the g^* curves for all α and y_w approach for large γ and small β, the asymptote $\gamma\beta = 1$ as in the laminar case. The uniquesness boundary (g^* and H^* curves) for the adiabatic case is given by

$$\gamma = \begin{cases} \dfrac{(1+\beta)(2+\beta)}{2\beta} & \text{for} \quad 0 < \beta < \sqrt{2} \\ 1.5 + \sqrt{2} & \text{for} \quad \beta > \sqrt{2} \end{cases} \tag{55}$$

For the thermal expansion case (Figures 4c and 5c) the g^* curves approach for small β values the asymptote

$$\gamma\beta = 0.5, \tag{56}$$

while for the adiabatic case the exact uniqueness boundary is given by

$$\gamma = \begin{cases} \dfrac{(1+\beta)^2}{2\beta} & \text{for} \quad 0 < \beta < 1 \\ 2 & \text{for} \quad \beta > 1 \end{cases} \tag{57}$$

In the turbulent and thermal expansion cases a H^* curve exists for all α and y_w so that thermoflow multiplicity exists only for activation energies larger than some critical value. The calculations, shown in Figures 4 and 5, and Eqs. 55 and 57 indicate that this limiting γ value is rather low and is exceeded by most industrial reactions.

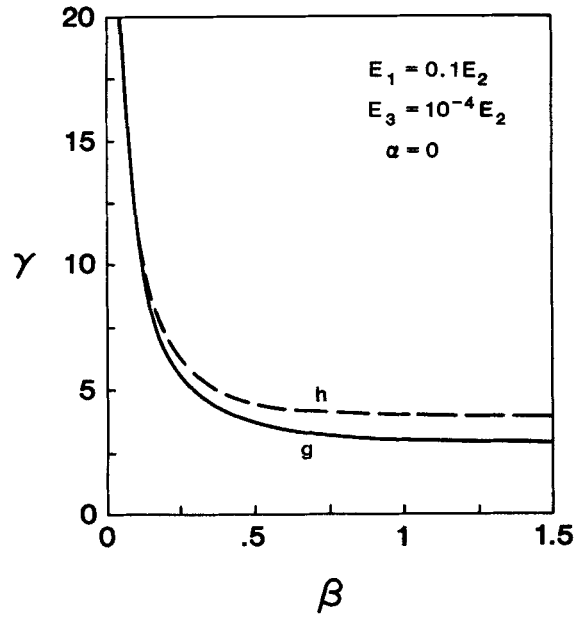

Figure 6. Thermoflow and thermokinetic (dashed) uniqueness boundaries for the general case of the lumped thermal model.

The g curve for the general case is bounded by those for the three limiting cases. Figure 4d shows these three curves for $\alpha = 1$. Clearly, the g curve for the general case is to the left (lower β values) of that for the turbulent case and to the right of that of the thermal expansion for small β, and above that for the laminar case for large β values.

Figure 6 shows a typical g curve for the general case. For all (γ, β) values to the left or below the g curve, the pressure drop is a monotonic increasing function of the inlet velocity. In other words, the inlet velocity is a monotonic increasing function of the pressure drop. For all (γ, β) to the right or above this curve thermoflow multiplicity exists, i.e., three different inlet velocities (Da) may exist for some specified pressure drop, or equivalently Λ_2. Two examples of such cases are shown in Figure 7.

Figure 6 describes also the h curve (thermokinetic boundary) which is the locus of the hysteresis variety of Eq. 44, defined by Eqs. 50a and 50b for the adiabatic case. For all (γ, β) values to the left or below this boundary a unique state exists for every specified Da, i.e., inlet velocity. For any (γ, β) values to the right or above this boundary three states exist for all Da values in (Da^*, Da^m), Figure 7b. The upper bound Da^m satisfies the relation

$$Da^m = \frac{y - 1}{\beta[X(y) - \alpha(y - y_w)]} \tag{58}$$

where y is the smallest of the two roots of Eq. 49. The lower bound Da^* is found by the simultaneous solution of Eqs. 45–46. Note that Da^m and Da^* are the same for the general case and the limiting cases as they are determined by equations which are independent of the momentum balance, and hence the pressure drop parameters, E_i.

When the thermokinetic multiplicity exists, complete conversion occurs only for one of the three states. Hence, the conversion is not complete for some states for which $Da > D_a^*$.

Figure 7b indicates that for a set of parameters above or to the right of the h curve, the bifurcation diagram of Da vs. Λ_2 exhibits both thermoflow multiplicity as well as thermokinetic multi-

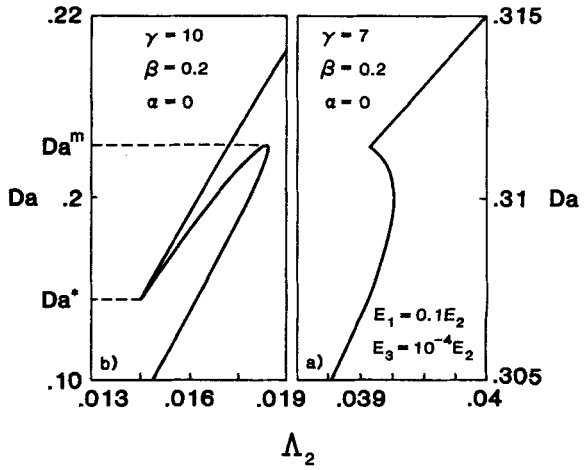

Figure 7. Bifurcation diagrams of Da vs. Λ_2 for the lumped-thermal model. In both cases thermoflow multiplicity exists. Thermokinetic multiplicity exists only in case b.

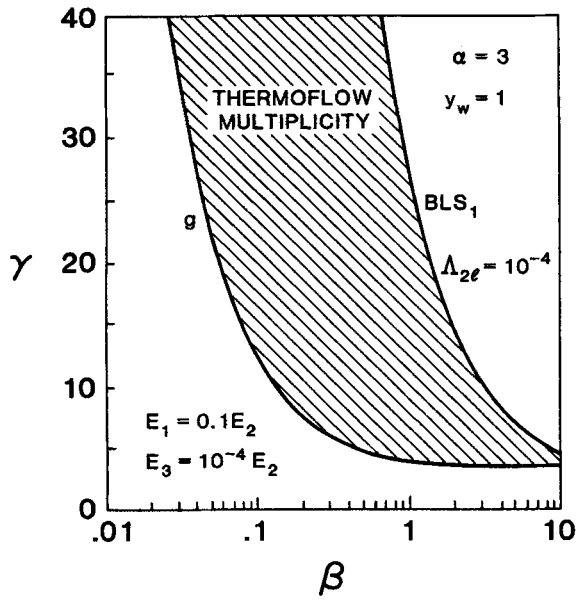

Figure 8. Region of (γ, β) values for which thermoflow multiplicity exists for the lumped-thermal model for $\Lambda_{2l} = 10^{-4}$.

plicity. Numerical simulations show that increasing α or decreasing coolant temperature, y_w, shrinks the gap between the g and h curves.

Thermoflow multiplicity occurs for some feasible pressure drop only for (γ, β) values to the right of the g curve and to the left of the BLS_1 curve, corresponding to the lowest allowable exit pressure. Figure 8 describes these two curves for a typical set of parameters. Thermoflow multiplicity can be found for some feasible exit pressure for all (γ, β) values bounded between these two curves. Comparison of this region with that found for the negligible axial dispersion model (Figure 3) shows that the lumped thermal model predicts that multiplicity occurs for lower (and much more realistic) values of β than does the negligible axial dispersion model. The calculations indicate that the BLS_1 for the lumped thermal model is usually slightly to the left (smaller β values) of that computed for the negligible axial dispersion model.

A comparison of the multiplicity region for the negligible dispersion model (Figure 3) with that for the lumped thermal model (Figure 8) indicates that the axial conductivity of heat increases significantly the region of (γ, β) values for which multiplicity can be found, especially for the realistic values of $\beta < 1$. Moreover, in the case of negligible dispersion the range of pressure drops, or equivalently of Λ_2, for which thermoflow multiplicity is found is very small, so that it will be hard to find in practice. However, in the case of the lumped-thermal model the multiplicity is observed over a very large range of exit pressures and is a robust phenomenon. For example, for $\gamma = 20$ and $\alpha = 0$ this ratio is 3.45×10^5, 1.02×10^8 and 2.56×10^{10} for β values of 1, 2 and 5, respectively. Note that the corresponding values of this ratio for the negligible dispersion model are 1.0003, 1.0014, and 1.0484, respectively.

Finite Heat Dispersion Model: Finite Pe_h

The large differences in the predictions of the limiting models of the negligible axial dispersion and lumped-thermal (infinite dispersion) about the existence of thermoflow multiplicity for realistic parameters indicate the importance of accounting properly for thermal dispersion of heat. There exists a certain disagreement among various investigators about the exact value of the Peclet number for effective thermal conductivity but it is generally agreed that its value (based on particle length) is of the order of 0.5 (Votruba et al., 1972). Thus the practical range of Peclet heat numbers (based on reactor length) is 50 to about 1,000. Axial feedback of heat may lead to multiplicity even for very large values of the Peclet numbers (Puszynski et al., 1981) and we investigate its impact on thermoflow multiplicity here.

The determination of the uniqueness boundary for the finite dispersion model defined by Eqs. 15–20 is more intricate than for the limiting models. It requires numerical computations of the singular points using the scheme described by Witmer et al. (1986) and is reported by Pita (1988). We focus here on the results and their implications.

Figure 9 describes the dependence of the hysteresis variety (g curves) on the thermal dispersion modulus ϕ_h^2 ($= Pe_h Da$) for an adiabatic reactor in which we account only for the turbulent pressure loss ($E_1 = E_3 = 0$). The negligible dispersion and lumped thermal models correspond to ϕ_h^2 values of ∞ and 0, respectively. The calculations show that for unrealistically large values of β all the g curves with finite Pe_h converge to that for the negligible dispersion model. The physical reason is that for large β and low activation energy the finite dispersion of heat does not have a strong impact on the g curves.

On the other hand, for realistically small values of β the curves converge to that of the lumped-thermal model for large γ. The reason is that the impact of the thermal feedback increases as the activation energy increases. The calculations clearly show that increasing the heat dispersion shifts the multiplicity boundary towards lower and more realistic β values. The value of the Damköhler number along the hysteresis variety is of order 0.1. Thus, the practical value of the axial conductivity modulus is of order 100. We therefore conclude from Figure 9 that the g curve for the lumped-thermal model is a much better approximation of the behavior for realistic β values than is the g curve for the

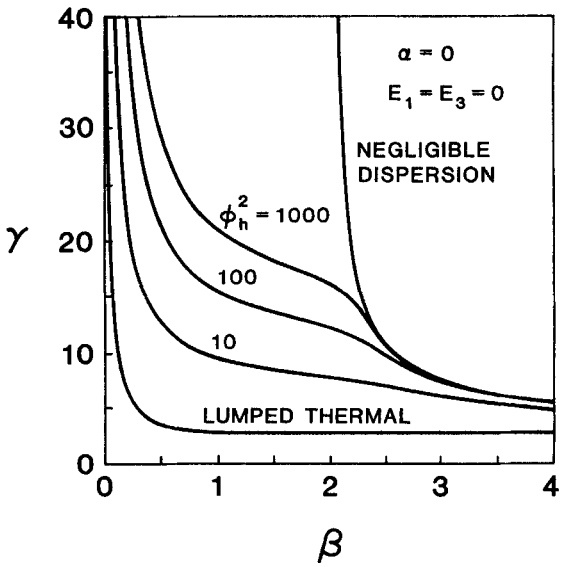

Figure 9. Dependence of the g (hysteresis) curves on the thermal conductivity modulus ϕ_h^2.

negligible dispersion model and that the finite axial conduction of heat enables thermoflow multiplicity to occur for realistic β values.

Consider a reaction with a specified γ value. Figure 9 indicates that a continuous increase of ϕ_h^2 increases the values of β on the hysteresis variety from that of the lumped-thermal model to that of the negligible dispersion model. Figure 10 describes this variation of β values as a function of Pe_h for several γ values. It is of interest to note that for $\gamma = 10$ (20) the value corresponding to the negligible dispersion model is approached asymptotically at Pe_h of about 10^4 (10^6). For all γ values larger than or equal to 30 the negligible dispersion model limit is not attained even for the unrealistically high value of $Pe_h = 10^6$. This underscores the fact that the negligible dispersion model is not an adequate approximate model for predicting thermoflow multiplicity.

The g and BLS_1 curves bound the (γ, β) values for which thermoflow multiplicity can be found for a specific Λ_{2l}. The calculations have shown that the BLS_1 curves are very close to those of the negligible dispersion model for realistic ϕ_h^2 values (>10). Figure 11 describes the BLS_1 for the two limiting models and $\phi_h^2 = 1$. The BLS_1 curves for all $\phi_h^2 > 1$ are bounded between this curve and that for the negligible dispersion model. They are not shown here due to the small separation between these two curves.

The largest difference in the β values of the g curves of the two limiting models is found for the turbulent case. Figure 12 describes the g curves of a cooled reactor for the general case ($E_1E_2E_3 \neq 0$). It is again seen that small but finite dispersion of heat shifts the g-curves towards that for the lumped thermal model, and allows thermoflow multiplicity to be found at lower β values. Numerical calculation shows that an increase in the ratio of E_3/E_2 tends to reduce the separation between the g-curves for the two limiting models. The ratio selected in this example is probably an upper bound for most industrial reactors.

Figure 13 describes the multiplicity region of the finite dispersion model for a typical set of parameters. For all (γ, β) values in the hatched region the Da vs. Λ_2 bifurcation diagram

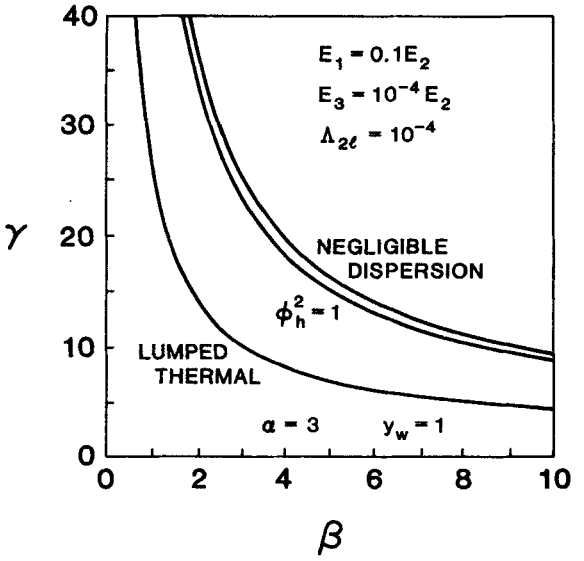

Figure 11. *BLS*, curves for the lumped-thermal and negligible dispersion models and for $\phi_h^2 = 1$ for a cooled reactor, general case.

exhibits thermoflow multiplicity for a range of Λ_2 values bounded between either the extinction and ignition values, Λ_{2e} and Λ_{2l}, or Λ_{2l} and Λ_{2i}. When the range $(\Lambda_{2e}, \Lambda_{2i})$ is narrow, as in the negligible dispersion model, the probability of observing this multiplicity is very small. The multiplicity is robust and easily observable when this range is wide and feasible.

Numerical calculations have shown that the range of $(\Lambda_{2e}, \Lambda_{2l})$ is very wide for the lumped thermal model. It still remains very large for the finite dispersion model for reasonable ϕ_h^2 values. The range in general tends to decrease as the thermal conductivity modulus is increased. The ignition and extinction do eventually coalesce in a cusp if the γ and β values are to the right of the g curve for the lumped thermal model and to the left

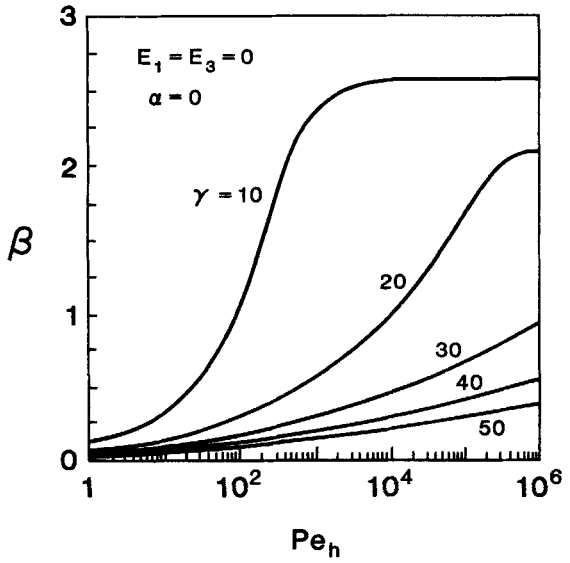

Figure 10. Dependence of β on the g (hysteresis) curve on Pe_h and γ for an adiabatic reactor, turbulent case.

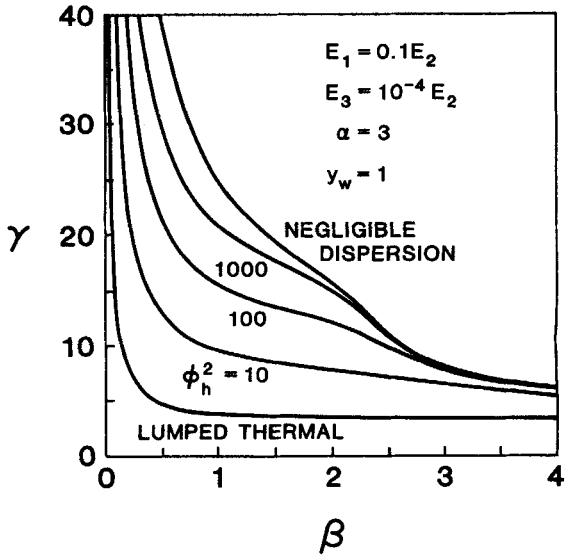

Figure 12. g (hysteresis) curves of a cooled reactor for the general case.

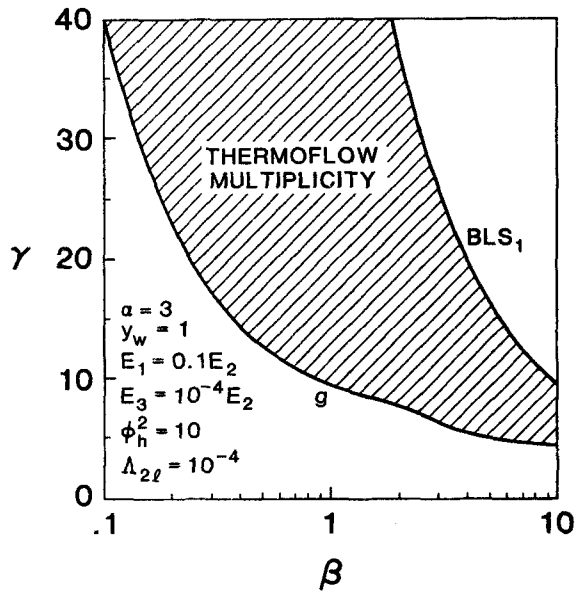

Figure 13. Region of (γ, β) values for which thermoflow multiplicity exists for a cooled reactor with finite dispersion.

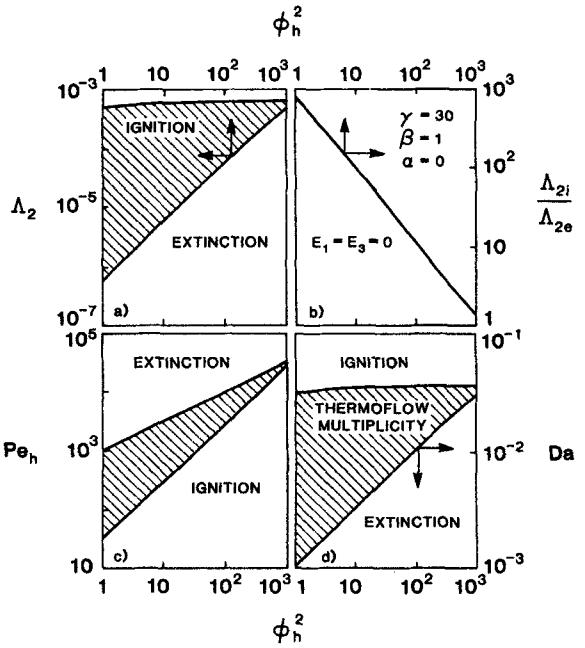

Figure 14. Dependence of Λ_2 (a), Pe_h (c), and Da (d) on ϕ_h^2 at the ignition and extinction loci on ϕ_h^2 for an adiabatic reactor and the turbulent case. The ratio of Λ_2 at ignition to that at extinction is shown in (b).

of that for the negligible dispersion model. Clearly, for all ϕ_h^2 values larger than those at the cusp point thermoflow multiplicity does not occur for any Λ_2. When the (γ, β) are to the right of the g curve for the negligible dispersion model the ignition and extinction loci do not intersect but approach each other as ϕ_h^2 is increased. In general, the two are rather close for the negligible dispersion model ($\phi_h^2 \to \infty$).

Figure 14a describes the loci of the ignition and extinction points of an adiabatic reactor and the limiting turbulent case as a function of the thermal conduction modulus for a set of parameters for which thermoflow cannot exist for the negligible dispersion model. The loci of the ignition and extinction point coalesce at a cusp (not shown in the figure) located at $\phi_h^2 = 3{,}250$, $Da = 0.036$, $Pe_h = 90{,}800$ and $\Lambda_2 = 6.17 \times 10^{-4}$. The graph indicates that a large multiplicity region exists for the practical cases in which ϕ_h^2 is smaller than 100.

Figure 14b shows the ratio between Λ_2 at the ignition and extinction point for various ϕ_h^2 values. This ratio decreases in almost a linear fashion in this logarithmic scale being 830 and 12 for ϕ_h^2 of 1 and 100. This ratio is equal to 3.3×10^9 for the lumped thermal model ($\phi_h^2 = 0$). This confirms the previous observation that thermoflow multiplicity occurs over a reasonable range of Λ_2 values, or equivalently exit pressure for typical parameters. Figure 14c describes the dependence of the Peclet number along the ignition and extinction loci on ϕ_h^2. The logarithmic dependence is essentially linear and indicates that the Peclet numbers at extinction are very large (larger than 1,000 for all $\phi_h^2 > 1$). Figure 14d shows that Da at the ignition point are rather independent of ϕ_h^2 and their value changes from 0.031 at $\phi_h^2 = 1$ to 0.036 at $\phi_h^2 = 100$. On the other hand, the Da at the extinction point increases almost linearly on this logarithmic graph and is equal to 1.05×10^{-3} and 10^{-2} for ϕ_h^2 of 1 and 100, respectively. In the lumped thermal model the Damkohler number is equal to 0.013 and 3.1×10^{-7} at the ignition and extinction points, respectively.

Figures 15a–d describe the behavior of a cooled reactor for the general case. The calculations show that in this case a multiplicity region exists for all ϕ_h^2 and that ignition and extinction branches do not coalesce. In fact, for the negligible dispersion model thermoflow multiplicity still exists over a very narrow range of Λ_2 ($\Lambda_{2i}/\Lambda_{2e} = 1.00014$). For all $\phi_h^2 \leq 1{,}000$ the diagrams shown in Figure 15 are very similar to those shown in Figure 14. Apparently, the tendency of the cooling to reduce the multiplicity region has been compensated for by the inclusion of the small contribution by the thermal expansion to the overall pressure change in the reactor. Figure 16 shows the numerically computed bifurcation diagrams of Da vs. Λ_2 and y_1 vs. Λ_2 for a typical set of parameters. These figures show that thermoflow multiplicity can be encountered under a practical set of parameters in a cooled reactor. Note that in this case the range of exist pressures (Λ_2) for which thermoflow multiplicity occurs is essentially the same as that for which thermokinetic multiplicity occurs.

Conclusions and Remarks

This work shows that thermoflow multiplicity is predicted to exist by both the limiting negligible dispersion and lumped thermal models as well as by the finite dispersion model. Considering the practical case in which the turbulent frictional loss is the major cause of pressure loss, thermoflow multiplicity exists in the negligible dispersion model only for unrealistic values of β (>2) and/or for a very narrow range of exit pressures. On the other hand, for the lumped thermal model thermoflow multiplicity exists for a wide region of practical values of γ and β and over a wide range of exit pressures.

The calculations show that for the axial dispersion model an increase in the value of ϕ_h^2 decreases the range of exit pressures

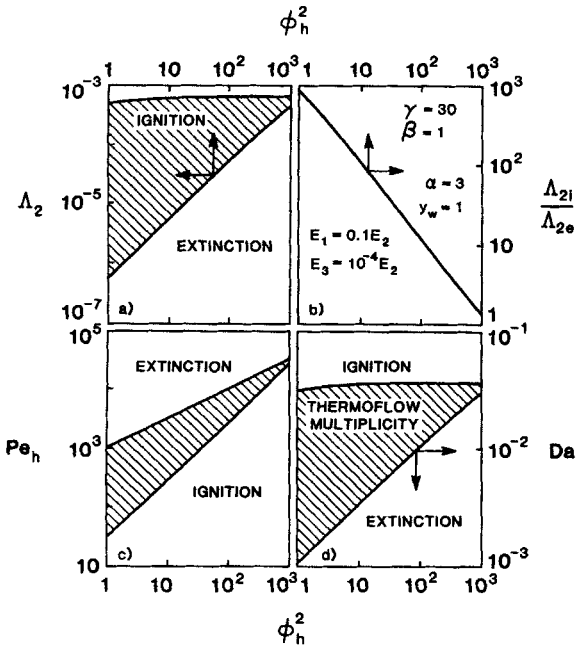

Figure 15. Dependence of Λ_2 (a), Pe_h (c), and Da (d) on ϕ_h^2 at the ignition and extinction loci on ϕ_h^2 for a cooled reactor and the general case. The ratio of Λ_2 at ignition to that at extinction is shown in (b).

over which thermoflow multiplicity occurs. However, for large values of ϕ_h^2, say of the order of 100, thermoflow multiplicity is found for practical values of γ and β and a reasonable range of exit pressures. Thus, the finite but small axial conduction of heat, which exists in industrial packed bed reactors, enables thermoflow multiplicity to exist under practical conditions. This may be a surprising result, as it is assumed in many places that the impact of this conduction can be ignored for large Peclet numbers. Our calculations show that this is definitely not the case.

The calculations also indicate that the thermal expansion of the gas, while having a relatively small contribution to the overall pressure change, tends to enhance the possible occurrence of

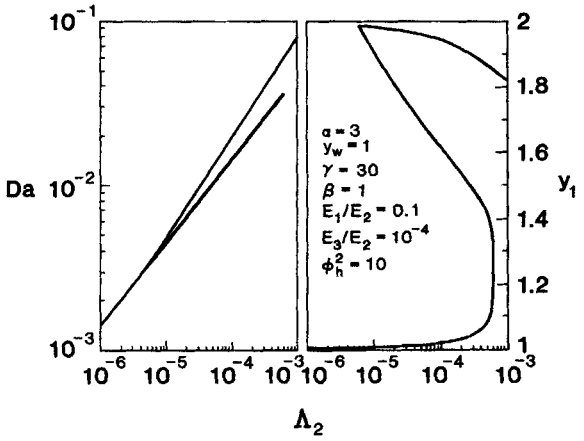

Figure 16. Bifurcation diagrams of Da vs. Λ_2 and y_1 vs. Λ_2 for a typical set of parameter values.

thermoflow multiplicity, and shifts the multiplicity region to lower and more realistic β values.

The calculations show that cooling tends to decrease somewhat the region of (γ, β) values for which thermoflow can be obtained and shifts it to larger β values. However, that impact is not very strong and, as seen by Figure 15, thermoflow multiplicity can exist with cooling under a realistic set of parameters.

This paper indicates that the presence of the small axial thermal conductivity in a packed bed reactor and the small impact of thermal expansion on the pressure change in the reactor enable thermoflow multiplicity to occur under practical conditions. Thus, it is important to check for its occurrence in the design of multitube reactors, as its presence can lead to undesired radial thermal gradients and corresponding mechanical stresses.

Acknowledgment

We would like to thank the National Science Foundation and the American Chemical Society-Petroleum Research Fund for support of this research.

Notation

A = constant for laminar contribution in Ergun equation
B = constant for turbulent contribution in Ergun equation
C_A = concentration of species A
c_p = heat capacity
Da = Damkohler number defined by Eq. 14
Da_u^m = upper bound Da defined by Eq. 58
Da = smallest Da for which conversion is complete
E = activation energy
E_1, E_2, E_3 = dimensionless parameters in momentum balance defined by Eq. 14
F = function defining steady state
F_1 = function defining steady state for incomplete conversion
F_2 = function defining steady state for complete conversion
f_p = frictional pressure drop gradient defined by Eq. 5
g^* = parameter set satisfying Eqs. 35a and 35b
g = curve represented by the union of segments g^* and H^*
H = heavyside's function
H^* = parameter set satisfying Eq. 36
ΔH = heat of reaction
h = wall heat transfer coefficient
I = function defined by Eq. 26
K = function defined by Eq. 33
$k(T)$ = reaction rate constant
L = length of reactor
P = pressure
$\mathbf{p}$ = parameters vector
Pe_h = heat Peclet number
R = universal gas constant
R_t = tube radius
r = reaction rate
s = dimensionless reactor length coordinate defined by Eq. 14
s_c = position at which conversion is complete
T = temperature
T_w = coolant temperature
t_c = characteristic convection time
t_λ = characteristic conduction time
u = velocity
X = function defined by Eq. 13
x = conversion
y = dimensionless temperature defined by Eq. 12
y_c = dimensionless temperature at which conversion is complete
y_w = dimensionless coolant temperature defined by Eq. 14
y_{wi} = dimensionless coolant temperature for isothermal operation defined by Eq. 22
z = reactor length coordinate

Greek letters

α = dimensionless heat transfer coefficient defined by Eq. 14
α_I = dimensionless heat transfer coefficient for isothermal operation defined by Eq. 21
β = adiabatic temperature rise defined by Eq. 14
β^* = β value corresponding to γ^*
γ = dimensionless activation energy defined by Eq. 14
γ^* = γ value satisfying Eq. 48
ϵ = small positive number in Eq. 35b
ϕ_h^2 = thermal conduction modulus defined by Eq. 14
Λ_j = parameter defined by Eq. 28, $j = 1, 2, 3$
λ_e = effective axial thermal conductivity
μ = viscosity
Π = dimensionless pressure defined by Eq. 14
ρ = density
θ = variable in Eq. 40 defined as $\theta = \gamma (y_1 - 1)$

Subscripts

l = limiting
0 = inlet to reactor
1 = outlet of reactor

Literature Cited

Lee, J. P., V. Balakotaiah, and D. Luss, "Thermoflow Multiplicity in a Packed-Bed Reactor: I. Adiabatic Case," *AIChE J.*, **33**, 1136 (1987).

Lee, J. P., V. Balakotaiah, and D. Luss, "Thermoflow Multiplicity in a Packed-Bed Reactor: II. Impact of Volume Change," *AIChE J.*, **34**, 37 (1988).

Matros, Yu. Sh., and N. A. Chumakova, "Multiplicity of Stationary Regimes in an Adiabatic Catalyst Layer," *Dokl Akad Nauk SSSR*, **250**(6), 1421 (1980).

Pita, J. A., "Thermoflow Multiplicity in Nonadiabatic Multitube Reactors," Ph.D. Thesis, University of Houston (1988).

Puszynski, J., D. Snita, V. Hlavacek, and H. Hofmann, "A Revision of Multiplicity and Parametric Sensitivity Concepts in Nonisothermal Nonadiabatic Packed Bed Chemical Reactors," *Chem. Eng. Sci.*, **36**, 1605 (1981).

Votruba, J., V. Hlavacek, and M. Marek, "Packed bed axial thermal conductivity," *Chem. Eng. Sci.*, **27**, 1845 (1972).

Witmer, G. S., V. Balakotaiah, and D. Luss, "Multiplicity Features of Distributed Systems: I. Langmuir-Himshelwood Reaction in a Porous Catalyst," *Chem. Eng. Sci.*, **41**, 179 (1986).

Manuscript received June 8, 1988, and revision received Oct. 17, 1988.